Stabilization of the cyclotron autoresonance maser instability by axial momentum spread

Ronald C. Davidson
Plasma Fusion Center, Massachusetts Institute of Technology, Cambridge, Massachusetts 02139

Peter H. Yoon
Center for Space Research, Massachusetts Institute of Technology, Cambridge, Massachusetts 02139
(Received 6 September 1988)

This paper investigates the stabilizing influence of axial momentum spread on the linear growth properties of the cyclotron autoresonance maser (CARM) instability. The stability analysis is based on the linearized Vlasov-Maxwell equations for a relativistic electron beam and right-circularly-polarized electromagnetic waves propagating parallel to a uniform magnetic field $B_0\hat{\mathbf{e}}_z$. Detailed stability properties are investigated for a choice of beam equilibrium $f_b^0(p_\perp^2,p_z)$ that incorporates both an inverted population in perpendicular momentum $p_\perp$ and a spread Δ in axial momentum p_z. For simplicity, the analysis neglects the influence of finite radial geometry ($k_\perp \to 0$ and no radial waveguide structure). The resulting dispersion relation is analyzed numerically in parameter regimes of interest for CARM applications, and approximate analytical estimates of the (reduced) growth rate are presented.

I. INTRODUCTION

Numerical-simulation studies and simple analytical estimates indicate that modest values of axial momentum spread[1-7] can have a large effect in reducing the growth rate and saturation efficiency of the cyclotron autoresonance maser (CARM) instability.[8,9] (See, for example, the numerical simulations[2] by Lin *et al.*, who investigated the effects of axial momentum spread on the growth rate of a CARM amplifier). It is therefore essential that CARM experiments operating in waveguide cavities utilize high-quality electron beams, or that alternate configurations be employed, which are less sensitive to momentum spread, such as in the induced resonance electron cyclotron (IREC) quasioptical maser.[1] The purpose of this paper is to quantify the stabilizing influence of axial momentum spread on the linear growth properties of the cyclotron autoresonance maser instability. The stability analysis is based on the linearized Vlasov-Maxwell equations for a relativistic electron beam and right-circularly-polarized electromagnetic waves propagating parallel to a uniform magnetic field $B_0\hat{\mathbf{e}}_z$. Detailed stability properties are investigated for a choice of beam equilibrium $f_b^0(p_\perp^2,p_z)$ [Eq. (3)] that incorporates both an inverted population in perpendicular momentum $p_\perp$ and a spread in axial momentum p_z. For simplicity, the analysis neglects the influence of finite radial geometry ($k_\perp \to 0$ and no radial waveguide structure). The resulting dispersion relation [Eq. (7)] is analyzed numerically, and approximate analytical estimates of the (reduced) growth rate are presented.

II. DISPERSION RELATION

For perturbation about a spatially uniform beam equilibrium $f_b^0(p_\perp^2,p_z)$, the dispersion relation for right-circularly-polarized electromagnetic waves propagating parallel to $B_0\hat{\mathbf{e}}_z$ can be expressed as[10]

$$0=D_T^-(k,\omega)$$
$$=\omega^2-c^2k^2-\omega_{pb}^2\int d^3p\,\frac{1}{\gamma}\left[\frac{\gamma\omega-kp_z/m}{\gamma\omega-kp_z/m-\omega_c}-\frac{p_\perp^2}{2m^2c^2}\frac{\omega^2-c^2k^2}{(\gamma\omega-kp_z/m-\omega_c)^2}\right]f_b^0(p_\perp^2,p_z)\,, \tag{1}$$

where k is the axial wave number and ω is the complex oscillation frequency, with $\mathrm{Im}\omega>0$ corresponding to instability. Here, $\omega_{pb}=(4\pi\hat{n}_b e^2/m)^{1/2}$ and $\omega_c=eB_0/mc$ are the nonrelativistic electron plasma and cyclotron frequencies, respectively, $\gamma=(1+\mathbf{p}^2/m^2c^2)^{1/2}$ is the relativistic mass factor, p_z is the axial momentum, and $p_\perp=(p_x^2+p_y^2)^{1/2}$ is the momentum perpendicular to $B_0\hat{\mathbf{e}}_z$. Moreover, $-e$ is the electron charge, m is the electron rest mass, c is the speed of light *in vacuo*, and the normalization of $f_b^0(p_\perp^2,p_z)$ is

$$\int d^3p\, f_{b0}=2\pi\int_0^\infty dp_\perp p_\perp\int_{-\infty}^\infty dp_z f_b^0=1\,.$$

The dispersion relation (1) neglects the influence of finite radial geometry and equilibrium self-field effects (tenuous-beam approximation). In the operating regimes of current practical interest for CARM's, the dimensionless quantity

$$\epsilon_b = \frac{\omega_{pb}^2}{\omega_c^2} \tag{2}$$

is typically a small parameter ($\epsilon_b \ll 1$).

For purposes of illustration, we consider the model distribution function (Fig. 1)

$$f_b^0 = \frac{1}{4\pi\hat{p}\Delta}\delta(p-\hat{p})\Theta((p_z-p_{zb})^2-\Delta^2) , \tag{3}$$

where $\hat{p}$, Δ, and p_{zb} are constants, $p=(p_\perp^2+p_z^2)^{1/2}$ is the total momentum, and $\Theta(x)$ is the Heaviside step function defined by $\Theta(x)=+1$ for $x<0$, and $\Theta(x)=0$ for $x>0$. Note from Fig. 1 that Eq. (3) incorporates an average axial drift (p_{zb}), a spread of (2Δ) in axial momentum p_z, and an inverted population in perpendicular momentum $p_\perp$, which drives the CARM instability associated with the fast-wave solution to Eq. (1). Denoting $\langle\Psi\rangle=(\int d^3p\,\Psi f_b^0)/(\int d^3p\,f_b^0)$, it readily follows from Eq. (3) that

$$\begin{aligned}
&\langle p_z\rangle = p_{zb} , \\
&\left\langle\frac{p_z}{\gamma m}\right\rangle = \frac{p_{zb}}{\hat{\gamma}m} \equiv V_b , \\
&\left\langle\frac{(p_z-\langle p_z\rangle)^2}{\gamma^2m^2c^2}\right\rangle = \frac{\Delta^2}{3\hat{\gamma}^2m^2c^2} \equiv \tfrac{1}{3}(\Delta\beta_z)^2 , \\
&\left\langle\frac{p_\perp^2}{\gamma^2m^2c^2}\right\rangle = \frac{\hat{p}^2-(p_{zb}^2+\Delta^2/3)}{\hat{\gamma}^2m^2c^2} \equiv \hat{\beta}_\perp^2-\tfrac{1}{3}(\Delta\beta_z)^2 ,
\end{aligned} \tag{4}$$

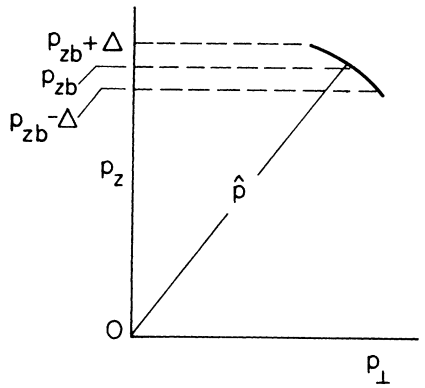

FIG. 1. Schematic of the distbribution function f_b^0 in Eq. (3). Electrons move on surface with $(p_\perp^2+p_z^2)^{1/2}=\hat{p}=$const. Average axial momentum is p_{zb}, and the axial momentum spread is 2Δ.

where $\hat{\gamma}\equiv(1+\hat{p}^2/m^2c^2)^{1/2}$ and $\hat{\beta}_\perp^2\equiv(\hat{p}^2-p_{zb}^2)/\hat{\gamma}^2m^2c^2$. In Eq. (4), $V_b\equiv p_{zb}/\hat{\gamma}m$ is the average axial velocity of the electron beam and $\Delta\beta_z\equiv\Delta/\hat{\gamma}mc$ is a measure of the normalized axial velocity spread associated with the distribution function in Eq. (3). Moreover, for sufficiently small momentum spread [$(\Delta\beta_z)^2\ll 3\hat{\beta}_\perp^2$], the quantity $\hat{\beta}_\perp c$ can be identified with the average speed of the electrons perpendicular to the magnetic field $B_0\hat{e}_z$.

Substituting Eq. (3) into Eq. (1) and carrying out the required integration over momentum, we obtain the dispersion relation for right-circularly-polarized electromagnetic waves, i.e.,

$$\begin{aligned}
0=D_T^-(k,\omega)=(\omega^2-c^2k^2)&\left[1-\frac{\omega_{pb}^2/\hat{\gamma}}{2c^2k^2}\left[\frac{(\omega-\omega_c/\hat{\gamma})^2-k^2\hat{p}^2/\hat{\gamma}^2m^2}{(\omega-kV_b-\omega_c/\hat{\gamma})^2-c^2k^2(\Delta\beta_z)^2}+1-\frac{2(\omega-\omega_c/\hat{\gamma})S_k}{\omega-kV_b-\omega_c/\hat{\gamma}}\right]\right] \\
&-\frac{\omega_{pb}^2}{\hat{\gamma}}\left[1+\frac{(\omega_c/\hat{\gamma})S_k}{\omega-kV_b-\omega_c/\hat{\gamma}}\right] .
\end{aligned} \tag{5}$$

Here $\Delta\beta_z\equiv\Delta/\hat{\gamma}mc$ and S_k is the logarithmic function defined by

$$S_k=-\frac{\omega-kV_b-\omega_c/\hat{\gamma}}{2ck\Delta\beta_z}\ln\left[\frac{\omega-kV_b-\omega_c/\hat{\gamma}-ck\Delta\beta_z}{\omega-kV_b-\omega_c/\hat{\gamma}+ck\Delta\beta_z}\right] . \tag{6}$$

The dispersion relation for left-circularly-polarized electromagnetic waves propagating parallel to $B_0\hat{e}_z$ is identical to Eq. (5), making the replacement $-\omega_c\to\omega_c$ in Eqs. (5) and (6). In the limit of zero momentum spread with $\Delta\beta_z\to 0$ [specifically, $c^2k^2(\Delta\beta_z)^2\ll|\omega-kV_b-\omega_c/\hat{\gamma}|^2$], we note from Eq. (6) that $S_k\simeq 1+\frac{1}{3}c^2k^2(\Delta\beta_z)^2/(\omega-kV_b-\omega_c/\hat{\gamma})^2+\cdots\to 1$. Making use of the definitions $\epsilon_b=\omega_{pb}^2/\omega_c^2$ and $\hat{\beta}_\perp^2=(\hat{p}^2-p_{zb}^2)/\hat{\gamma}^2m^2c^2$, and rearranging terms in Eq. (5), it is straightforward to show that the dispersion relation can be expressed in the equivalent form

$$\begin{aligned}
\frac{\omega^2-c^2k^2}{\omega_c^2}&\left\{1+\frac{1}{2}\frac{\epsilon_b}{\hat{\gamma}}\frac{\omega_c^2}{(\omega-kV_b-\omega_c/\hat{\gamma})^2-c^2k^2(\Delta\beta_z)^2}\left[\hat{\beta}_\perp^2-(\Delta\beta_z)^2\left[1+\frac{2kV_b}{\omega-kV_b-\omega_c/\hat{\gamma}}\right]\right]\right\} \\
&=\frac{\epsilon_b}{\hat{\gamma}}\left[\frac{\omega-kV_b}{\omega-kV_b-\omega_c/\hat{\gamma}}+\frac{(\omega_c/\hat{\gamma})(S_k-1)}{\omega-kV_b-\omega_c/\hat{\gamma}}\left[1-\frac{\omega^2-c^2k^2}{c^2k^2}\frac{\omega-\omega_c/\hat{\gamma}}{\omega_c/\hat{\gamma}}\right]\right] .
\end{aligned} \tag{7}$$

The form of the dispersion relation (7), which is exactly equivalent to Eq. (5), clearly delineates the effects of momentum spread through the factors proportional to $(\Delta\beta_z)^2=\Delta^2/\hat{\gamma}^2m^2c^2$ and S_k-1. Indeed, for $\Delta\to 0$, Eq. (7) reduces to the familiar Chu-Hirshfield dispersion relation[10,11] for the cyclotron maser instability, extended to the case of an electron beam drifting with axial velocity V_b.

III. ANALYSIS OF STABILITY PROPERTIES

Equation (7), which we refer to as the *full dispersion relation* (FDR), can be solved numerically (see below) and used to evaluate detailed properties of the cyclotron maser instability over a wide range of system parameters ϵ_b, $\hat{\beta}_\perp^2$, $(\Delta\beta_z)^2$, etc. For ϵ_b of order unity, all of the terms in Eq. (7) usually compete in determining the real oscillation frequency $\mathrm{Re}\omega$ and growth rate $\mathrm{Im}\omega$. For $\epsilon_b \ll 1$, however, which is the regime of practical interest[6] for CARM devices (where ϵ_b is typically in the range of 10^{-2}), the full dispersion relation (7) can be simplified to give an approximate dispersion relation that is analytically tractable. Specifically, for $\epsilon_b \ll 1$ and sufficiently small $\Delta\beta_z$, the frequency and wave number of the cyclotron maser branch in Eq. (7) satisfy

$$|\omega - kV_b - \omega_c/\hat{\gamma}|^2 \lesssim \tfrac{1}{2}\frac{\epsilon_b}{\hat{\gamma}}\hat{\beta}_\perp^2\omega_c^2 ,$$
$$|kV_b|(\Delta\beta_z)^2 \ll \tfrac{1}{2}\hat{\beta}_\perp^2|\omega - kV_b - \omega_c/\hat{\gamma}|$$
$$\lesssim \left[\frac{1}{8}\frac{\epsilon_b}{\hat{\gamma}}\right]^{1/2}\hat{\beta}_\perp^3\omega_c . \tag{8}$$

Making use of Eqs. (6) and (8), a careful examination of Eq. (7) shows that the dispersion relation for the cyclotron maser instability can be approximated to leading order by

$$(\omega^2 - c^2k^2)\left\{[(\omega - kV_b - \omega_c/\hat{\gamma})^2 - c^2k^2(\Delta\beta_z)^2] + \frac{1}{2}\frac{\epsilon_b}{\hat{\gamma}}\omega_c^2\hat{\beta}_\perp^2\right\} = 0 , \tag{9}$$

where the right-hand side of Eq. (9) includes contributions of order $\omega_c^4\epsilon_b^{3/2}\hat{\beta}_\perp$ and $\omega_c^4\epsilon_b^{1/2}(kV_b/\hat{\beta}_\perp\omega_c)(\Delta\beta_z)^2$. While the full dispersion relation (7) can be solved numerically in the region of interest for CARM applications, Eq. (9) constitutes a simple *reference dispersion relation* (RDR) with which to compare the more precise numerical results.

Equation (9) clearly illustrates the stabilizing influence of increasing the axial velocity spread $\Delta\beta_z = \Delta/\hat{\gamma}mc$. For $\Delta\beta_z = 0$, Eq. (9) gives

$$\mathrm{Re}\omega = kV_b + \omega_c/\hat{\gamma} ,$$
$$\mathrm{Im}\omega = \left[\frac{1}{2}\frac{\epsilon_b}{\hat{\gamma}}\right]^{1/2}\hat{\beta}_\perp\omega_c \equiv \Gamma_b , \tag{10}$$

for the unstable branch with $\mathrm{Im}\omega > 0$. On the other hand, for finite $(\Delta\beta_z)^2 \le (\epsilon_b/2\hat{\gamma})(\omega_c^2/c^2k^2)\hat{\beta}_\perp^2$, the approximate dispersion relation (9) gives

$$\mathrm{Re}\omega = kV_b + \omega_c/\hat{\gamma} ,$$
$$\mathrm{Im}\omega = \Gamma_b\left[1 - \frac{c^2k^2(\Delta\beta_z)^2}{\Gamma_b^2}\right]^{1/2} . \tag{11}$$

Therefore, for specified wave number k, Eqs. (9) and (11) predict that the maser instability is completely stabilized ($\mathrm{Im}\omega = 0$) whenever

$$c^2k^2(\Delta\beta_z)^2 \ge \Gamma_b^2 \equiv \frac{1}{2}\frac{\epsilon_b}{\hat{\gamma}}\hat{\beta}_\perp^2\omega_c^2 . \tag{12}$$

Typically, the CARM excitation wave number is somewhat less than the wave number $\hat{k} = (\omega_c/c\hat{\gamma})/(1 - V_b/c)$ determined from the intersection of the light line ($\hat{\omega} = c\hat{k}$) with the beam-cyclotron resonance condition ($\hat{\omega} = \hat{k}V_b + \omega_c/\hat{\gamma}$). If we estimate $k^2 \sim \hat{k}^2$ in Eq. (12), then stabilization occurs whenever

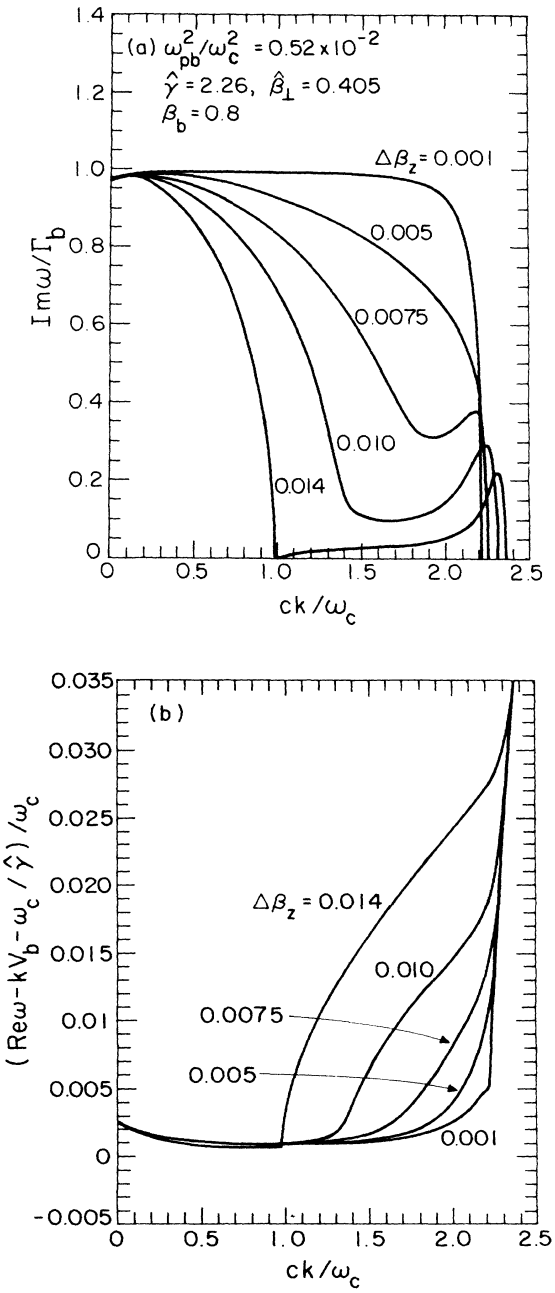

FIG. 2. Plots vs ck/ω_c of (a) $\mathrm{Im}\omega/\Gamma_b$ and (b) $(\mathrm{Re}\omega - kV_b - \omega_b/\hat{\gamma})/\omega_c$ obtained numerically from the full dispersion relation (7) for system parameters specified in Eq. (14), and $\Delta\beta_z = 0.001$, 0.005, 0.0075, 0.010, and 0.014.

$$(\Delta\hat{\beta}_z)^2 \gtrsim \tfrac{1}{2}\epsilon_b \hat{\beta}_\perp^2 \hat{\gamma}(1-\beta_b)^2 , \tag{13}$$

where $\beta_b \equiv V_b/c$, $\hat{\gamma} \equiv (1+\hat{p}^2/m^2c^2)^{1/2} = (1-\beta_b^2-\hat{\beta}_\perp^2)^{1/2}$, and $\Delta\beta_z = \Delta/\hat{\gamma}mc$. For $\epsilon_b \ll 1$ and $k^2 \lesssim \hat{k}^2$, it is evident from Eq. (13) that only a modest spread is required for stabilization.

As an illustrative example, we consider the choice of system parameters[6]

$$\epsilon_b = \omega_{pb}^2/\omega_c^2 = 0.52\times10^{-2},\ \hat{\gamma}=2.26 ,$$
$$\hat{\beta}_\perp = 0.405,\ \beta_b = 0.8 , \tag{14}$$

which corresponds to a maximum growth rate $\Gamma_b \equiv (\epsilon_b/2\hat{\gamma})^{1/2}\hat{\beta}_\perp\omega_c = 0.014\omega_c$, and $c\hat{k}/\omega_c \equiv (1/\hat{\gamma})/(1-\beta_b) = 2.21$. According to Eq. (13), significant growth-rate reduction already occurs when $\Delta\beta_z > 0.62\times10^{-2}$. The full dispersion relation (7) and the (approximate) reference dispersion relation (9) have been solved numerically over a wide range of system parameters. Typical results are summarized in Figs. 2 and 3 for the choice of parameters in Eq. (14). Shown in Fig.

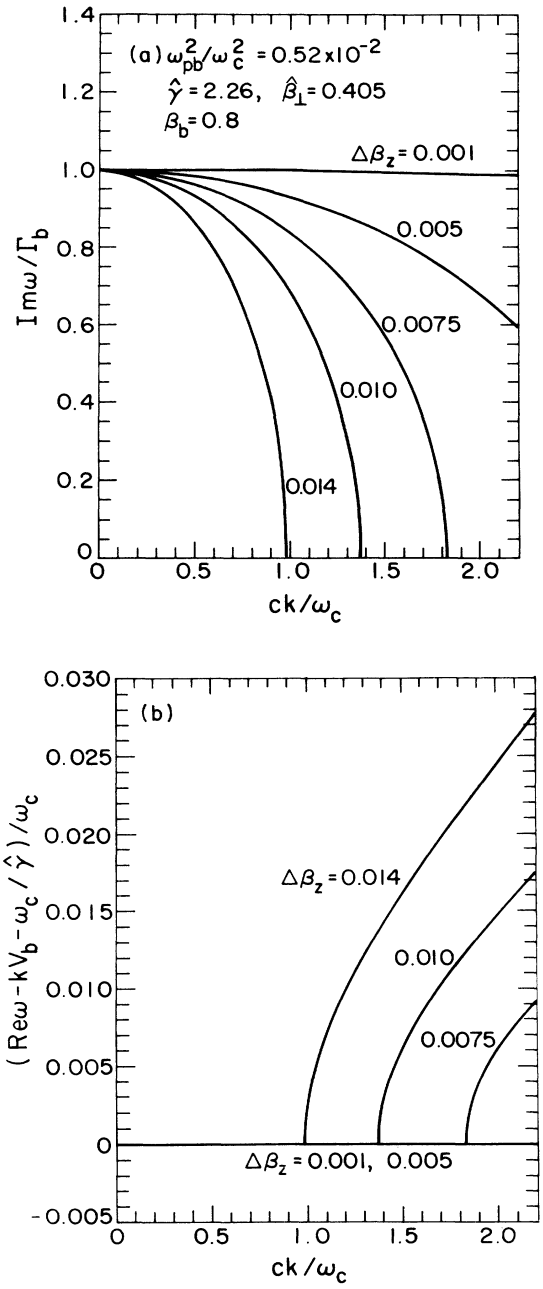

FIG. 3. Plots vs ck/ω_c of (a) $\mathrm{Im}\omega/\Gamma_b$ and (b) $(\mathrm{Re}\omega - kV_b - \omega_c/\hat{\gamma})/\omega_c$ obtained numerically from the reference dispersion relation (9) for system parameters specified in Eq. (14), and $\Delta\beta_z = 0.001$, 0.005, 0.0075, 0.0010, and 0.014.

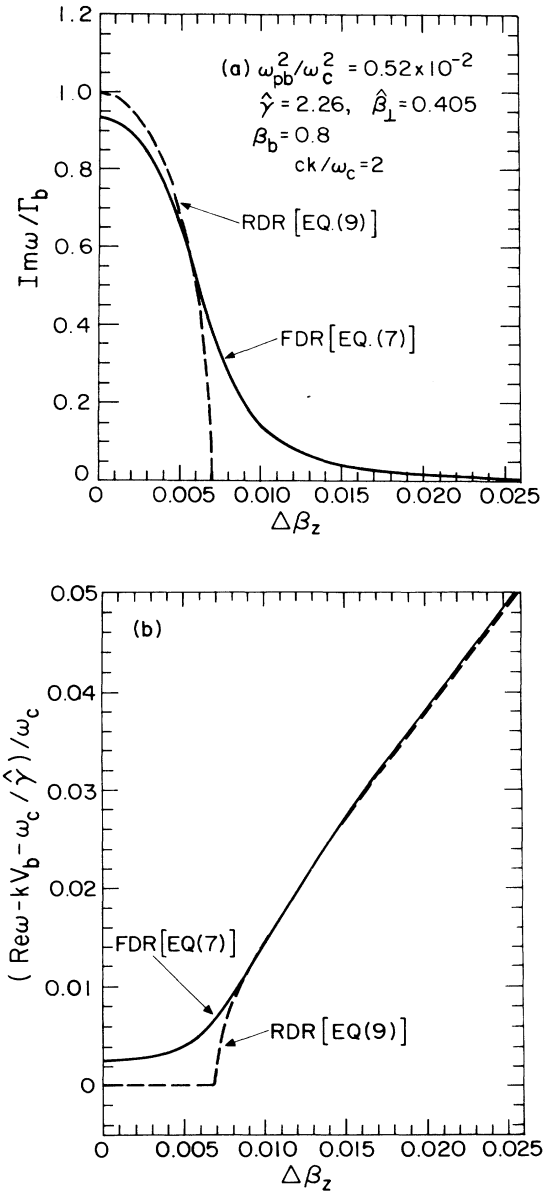

FIG. 4. Plots vs $\Delta\beta_z$ of (a) $\mathrm{Im}\omega/\gamma_b$ and (b) $(\mathrm{Re}\omega - kV_b - \omega_c/\hat{\gamma})/\omega_c$ obtained numerically from Eq. (7) (solid curves) and Eq. (9) (dashed curves) for fixed $ck/\omega_c = 2$ and system parameters specified in Eq. (14).

2 are plots versus ck/ω_c of the normalized growth rate $\mathrm{Im}\omega/\Gamma_b$ [Fig. 2(a)] and the real oscillation frequency $(\mathrm{Re}\omega - kV_b - \omega_c/\hat{\gamma})/\omega_c$ [Fig. 2(b)] obtained numerically from the full dispersion relation (7) for values of axial velocity spread corresponding to $\Delta\beta_z = 0.001$, 0.005, 0.0075, 0.010, and 0.014. Figure 3 presents plots versus ck/ω_c of $\mathrm{Im}\omega/\Gamma_b$ [Fig. 3(a)] and $(\mathrm{Re}\omega - kV_b - \omega_c/\hat{\gamma})/\omega_c$ [Fig. 3(b)] obtained numerically from the reference dispersion relation (9) for the same choice of parameters as in Fig. 2. Comparing Fig. 2(a) and Fig. 3(a), we note that $\mathrm{Im}\omega = \Gamma_b$ gives a good analytical estimate of the *maximum* growth rate [Eq. (10)].

As a general remark, it is evident from both Fig. 2 and Fig. 3 that only modest values of axial velocity spread $\Delta\beta_z$ are required to cause a substantial reduction in the growth rate $\mathrm{Im}\omega$ of the cyclotron maser instability. Moreover, as expected, the larger values of wave number k (shorter wavelengths) are most easily stabilized as $\Delta\beta_z$ is increased. For example, if we take the excitation wave number to be $ck/\omega_c = 2$, then the full dispersion relation (7) [Fig. 2(a)] predicts that the growth rate $\mathrm{Im}\omega$ decreases from $0.92\Gamma_b$, to $0.65\Gamma_b$, to $0.14\Gamma_b$, as $\Delta\beta_z$ is increased from 0.001, to 0.005, to 0.01, respectively. Similarly, for $ck/\omega_c = 2$, the reference dispersion relation 9 [Fig. 3(a)] predicts that $\mathrm{Im}\omega$ decreases from $0.99\Gamma_b$, to $0.69\Gamma_b$, to 0, as $\Delta\beta_z$ is increased from 0.001, to 0.005, to 0.01, respectively.

Comparing Figs. 2 and 3, it is evident that the reference dispersion relation (9) does not accurately predict the detailed structure and (small) magnitude of the growth rate $\mathrm{Im}\omega$ in the region near $k \sim \hat{k} = 2.12\omega_c/c$. Specifically, the logarithmic terms proportional to $S_k - 1$ in Eq. (7) result in the secondary growth-rate peaks in Fig. 2(a) for $\Delta\beta_z = 0.01$ and $\Delta\beta_z = 0.014$. A corresponding discrepancy is also apparent in the values obtained for $\mathrm{Re}\omega - kV_b - \omega_c/\hat{\gamma}$ [compare Fig. 2(b) and Fig. 3(b)].

Nonetheless, the reference dispersion relation (9) and Fig. 3 do give a good qualitative description of the growth-rate reduction produced by increasing the axial velocity spread $\Delta\beta_z$. Indeed, comparing Fig. 2(a) and Fig. 3(a), the reference dispersion relation (9) provides a good quantitative estimate of $\mathrm{Im}\omega$ whenever k is somewhat below $\hat{k} = 2.21\omega_c/c$ ($k < 0.9\hat{k}$, say) and the growth rate is sufficiently robust ($\mathrm{Im}\omega > 0.15\Gamma_b$, say). This is further illustrated in Fig. 4, where $\mathrm{Im}\omega/\Gamma_b$ and $(\mathrm{Re}\omega - kV_b - \omega_c/\hat{\gamma})/\omega_c$, calculated from Eqs. (7) and (9), are plotted versus $\Delta\beta_z$ for the choice of parameters in Eq. (14) and fixed value of $ck/\omega_c = 2$. Note from Fig. 4(a) that the full dispersion relation (7) predicts substantial growth rate reduction to $\mathrm{Im}\omega < 0.02\Gamma_b$ for $\Delta\beta_z > 0.02$.

ACKNOWLEDGMENTS

This work was supported in part by the Office of Naval Research, the Naval Research Laboratory Plasma Physics Division, and the Department of Energy High Energy Physics Division.

[1]P. Sprangle, C. M. Tang, and P. Serafim, App. Phys. Lett. **49**, 1154 (1986); Nucl. Instrum. Methods Phys. Res. **A250**, 361 (1986).

[2]A. T. Lin, K. R. Chu, and A. Bromborsky, IEEE Trans. Electron Devices **ED-34**, 2621 (1987).

[3]A. T. Lin and C. C. Lin, Phys. Fluids, **29**, 1348 (1986).

[4]A. W. Fliflet, Int. J. Electron. **61**, 1049 (1986).

[5]J. K. Lee, W. D. Bard, S. C. Chiu, R. C. Davidson, and R. R. Goforth, Phys. Fluids **31** (to be published).

[6]B. G. Danly, K. D. Pendergast, R. J. Temkin and J. A. Davies, Proc. SPIE **873** (to be published).

[7]K. Pendergast, B. G. Danly, R. Temkin, and J. S. Wurtele, IEEE Trans. Plasma Sci. **PS-18** (to be published).

[8]V. L. Bratman, N. S. Ginzburg, G. S. Nusinovich, M. I. Fetelin, and P. S. Strelkov, Int. J. Electron. **51**, 541 (1981).

[9]I. E. Botvinnik, V. L. Bratman, A. B. Volkov, G. G. Denisov, B. D. Kolchugin, and M. M. Ofitserov, Pis'ma Zh. Tekh. Fiz. **8**, 1386 (1982) [Sov. Tech. Phys. Lett. **8**, 596 (1982)].

[10]P. H. Yoon and R. C. Davidson, Phys. Rev. A **35**, 2619 (1987).

[11]K. R. Chu and J. L. Hirshfield, Phys. Fluids **21**, 461 (1978).